MODELING AND SIMULATION OF THE HEART´S TEMPERATURE DISTRIBUTION IN CARDIAC SURGERIES AS A FUNCTION OF THE CORONARY BLOOD FLOW

Fernando Gallego Dias, gallego@ufpr.br
José Viriato Coelho Vargas, jvargas@demec.ufpr.br
Marcos Leal Brioshi, termometria@yahoo.com.br
Programa de Pós Graduação em Engenharia - PIPE - UFPR, Caixa Postal 19011, Curitiba, PR, 81531-990, Brazil

Juan Carlos Ordonez, ordonez@caps.fsu.edu
Rob Hovsapian, hovsapian@caps.fsu.edu

CAPS – Center for Advanced Power Systems, 2000 Levy Ave, Tallahassee, FL, 32310

Abstract. *This work develops a theoretical and experimental analysis, the mathematical modeling, simulation and evaluation of the heart, during a cardiac surgery, through temperature data collection in real time surgery and the application of an alternative simulation technique, namely, the volume element model. The technique is based on the combination of classical thermodynamics and heat transfer principles, with the utilization of theoretical and empirical analytical correlations available in the literature. Using known coronary flows as input data, the work applies the volume element model to simulate the heart thermal response during open chest surgery, and, consequently, with the cardiac organ exposed to the external ambient. An experimental validation procedure of the obtained numerical results was conducted by direct comparison with the surface temperature measurements of the tissues via infrared camera images, in two distinct cases of cardiovascular obstructions. The numerical results showed very good qualitative and quantitative agreement with the two experimental measurements considered. Therefore, it is expected that the developed computational code, as the basis of a follow up work, will become a software to be utilized during cardiac surgeries to evaluate the organ reperfusion.*

Keywords*: heart model, heart thermal distribution, heart thermography, volume elements*

1. INTRODUCTION

The evaluation of the current perfusion at the trans-operatory insertion of cardiac grafts is a challenge yet to be solved. Various methods of evaluating the flow and muscle perfusion through grafts have been exhaustively tested without any success. Technically, when evaluating the flow alone through the graft, the surgeon faces the challenge if this flow wont´t necessarily mean good perfusion at the myocardium itself.

To evaluate the quality of the graft´s surgical connection, Robicsek et al. (1978) discovered, in a qualitative analysis, that the temperature of the heart´s surface is directly proportional to the coronary flow, which is also directly proportional to the infrared radiation emitted by the heart´s surface. After that, Papp et al. (1985) evaluated quantitatively the blood flow passing through the myocardial surface compared to the temperate distribution of the heart´s surface (epicardial temperature), and their preliminary results indicated that the temperature of the surface of the heart is strongly related with changes in the coronary blood flow rate.

Gordon et al. (1998) proposed the first quantitative model that tried to correlate, during a cardiac surgery with cooling of the heart, the coronary flow of the left anterior descending (LAD) branch of the left coronary with the average epicardial temperature acquired with an infrared camera. Such model proposed an exponential correlation between LAD flow and epicardial temperature, and, although being valid only for a very limited range of variation, was a good initial quantitative approach. Following that idea, Sterk and Trobee (2005) developed a simulation with high level of detailing for the same correlation problem, but with the downside of being extremely computing demanding, so demanding a very high computational time with parallel processing for solving each timeframe of correlation.

Recently, using the volume elements method, Vargas and Bejan (2004) and Vargas et. al. (2004) presented and developed the simulation and optimization of hydrogen fuel cells´ internal structures, showing that such method is very good for complex simulations of heat transfer, and also presents a significant reduced computational time.

In this context, this work presents the development and analysis of a volume element method for evaluating the distribution of the heart´s epicardial temperature in a cardiac surgery, with complete thoracotomy, as a function of the coronary blood flow, and validates such method comparing its results with real surgery results.

2. MATHEMATICAL MODEL

The problem consists in the calculation of the temperature distribution inside the chest and surrounding air. The mathematical domain, presented on Fig. 1a, is composed by a portion of the body, a portion of the surrounding air of the

operation room, and the complete heart, with its half exposed to the operation room, and the other half in contact with the warm mediastinum. A finite tri-dimensional volume method with centered cells was used to discretize the domain and solve the problem numerically (Fletcher, 1991). The novelty in the presented model is in the dimensions of the control volumes, which don´t need to be extremely reduced or differentials in order to obtain precise results, as it is commonly required by other numerical method, especially in the presence of a vast diversity of materials: muscles, air and blood interacting in the solution domain. The technique consist in dividing the box presented on Fig. 1a in small control volumes that contains only one type of element (air, muscle or blood), as shown in Fig. 1b, as well as calculating its interactions with its neighbors. The advantage in this approach is that, with a relatively small number of elements, it is possible to converge the solution with reduced computational time.

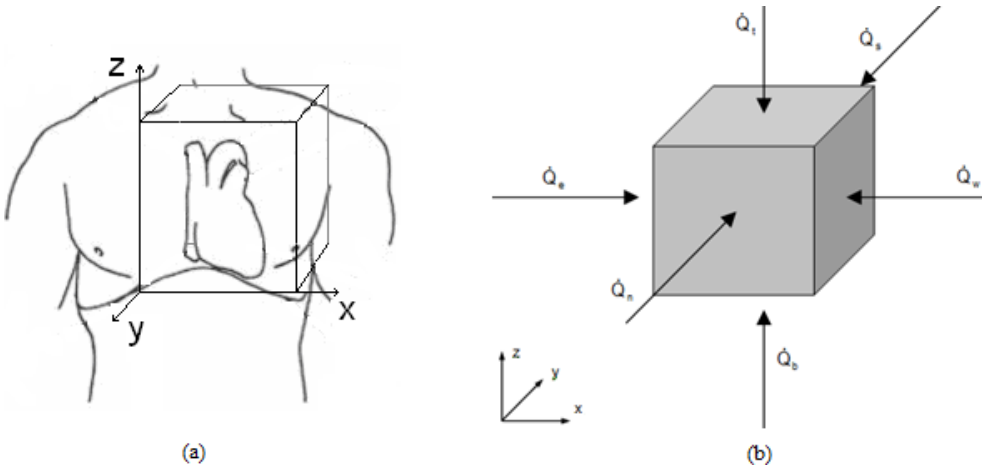

Figure 1. Computational domain (a) and representation of a single control volume element (b)

Applying the energy conservation (first law of thermodynamics) for each control volume will result Eq.(1), where T_i is the temperature in the center of each element, K, ρ is the specific mass of the material inside the element, kg/m^3, V is the volume of the element, m^3, c is the specific heat of the element, J/kg.K, $\dot{Q}_e, \dot{Q}_w, \dot{Q}_t, \dot{Q}_b, \dot{Q}_n$ and $\dot{Q}_s$ are the heat flow rates through the east, west, top, bottom, north and south walls respectively, W, $\dot{Q}_{gen}$ and $\dot{Q}_{vap}$ are the heat transfer rate due the heat generation inside the muscle elements, and the heat loss transfer rate of the muscle in contact with the operation room environment due the water evaporation, W.

$$\frac{dT_i}{dt} = \frac{1}{(\rho Vc)_i}[\dot{Q}_e + \dot{Q}_w + \dot{Q}_t + \dot{Q}_b + \dot{Q}_n + \dot{Q}_s + \dot{Q}_{gen} + \dot{Q}_{vap}]_i \text{, } 1 \le \text{i} \le \text{N} \quad (1)$$

As explained before, each element can be filled with air, blood or muscle. So, the heat transfer heat will be calculated depending on the actual material of the element, and in the material of its neighbor at the evaluated adjacent wall. In this simulation, the air is considered moving only for top or bottom interactions (vertical air flow), so for air/air lateral interactions, it is only considered heat conduction. The general equation for lateral air/air, and for air/muscle, air/blood, muscle/muscle and muscle/blood will the Eq. (2), where $\dot{Q}_{l,i}$ represents the heat transfer rate of the ith element in the direction l (east, west, north, south, top or bottom), W, $U_{l,i}$ represents the heat transfer coefficient between the adjacent elements, W/m^{2}K, $A_{l,i}$ represents their area of contact, m^2, and T_a represents the adjacent neighbor´s temperature, K.

$$\dot{Q}_{l,i} = -U_{l,i} A_{l,i} (T_i - T_a) \quad (2)$$

The heat transfer coefficient, $U_{l,i}$, will the calculated depending on the type of interaction: Air/air lateral contact will be ruled by Eq. (3), and muscle/muscle by Eq. (4). For air/muscle, blood/muscle or air/blood contact, Eq. (5) will be used, and for this equation, the convection heat transfer coefficient, h_l, will be calculated according to: Eq. (6) for natural convection with heat generation, Eq. (7) for natural convection without heat generation and Eq. (8) for forced convection with blood elements involved (Churchill and Chu, 1975). For these equations, k is the thermal conductivity of the material, W/m.K, d is length of the element in the evaluated direction, m, Re is the Reynolds number, Ra is the

Rayleigh number, Pr is the Prandtl number, g is the acceleration due to gravity, m^2/s, ν_a is the air´s kinematic viscosity, Pa.s, α is the air´s thermal diffusivity, m^2/s, and β is the air´s thermal expansion coefficient, K^{-1}.

$$U_{l,i} = \frac{k_{air}}{(d_i + d_a)/2}, \tag{3}$$

$$U_{l,i} = \frac{1}{\frac{d_i/2}{k_i} + \frac{d_a/2}{k_a}} \tag{4}$$

$$U_{l,i} = \frac{1}{\frac{1}{h_l} + \frac{d_i/2}{k_i}}, \tag{5}$$

$$h_l = \frac{k_{ar}}{d_i}\left\{0{,}825 + \frac{0{,}387 Ra_l^{1/6}}{\left[1+\left(\frac{0{,}437}{Pr}\right)^{9/16}\right]^{8/27}}\right\}^2 \tag{6}$$

$$h_l = \frac{k_{air}}{d_i}\left\{0{,}825 + \frac{0{,}387 Ra_l^{1/6}}{\left[1+\left(\frac{0{,}492}{Pr}\right)^{9/16}\right]^{8/27}}\right\}^2, \text{ with } Ra_l = \frac{g\beta}{\alpha\nu_a} d_i^3 \left|T_i - T_a\right| \tag{7}$$

$$h_i = \frac{k_{blood}}{L}\left(0.037\ Pr^{1/3}\ Re_L^{4/5}\right), \tag{8}$$

For air/air vertical contact or blood/blood contact, Eq. (9) will be used, where, in the case of air/air vertical contact, Eq. (10) will be used to calculated the average air vertical velocity, V_i, in m/s (Bejan, 1995a). For Eq. (9), $\dot{m}_{l,i}$ is the mass flow rate of the fluid at the ith element flowing at the direction l, Kg/s.

$$\dot{Q}_{l,i} = \dot{m}_{l,i} c_{p,fluid}(T_a - T_i), \text{ where } \dot{m}_{l,i} = \rho_{fluid} V_i \frac{A_{l,i}}{2} \tag{9}$$

$$V_i = \alpha\left(\frac{g\beta}{\alpha\nu}\left|T_a - T_i\right| d_i\right)^{1/2} \tag{10}$$

For the calculation of the heat transfer rate due to water evaporation in the surface of the exposed heart´s muscle, Eqs (11) – (14) will be used. In this case ρ_w represents the density of water vapor in the surface of the muscle, and ρ_∞ represents the density of water vapor outside in the operating room, Kg/m^3, both calculated according to equations (12) and (13). $\overline{h}_m$ is the average mass transfer coefficient, m/s, and can be calculated according to equation (14) (Bejan, 1993). h_{fg} is the water latent heat of vaporization, J/Kg, $\dot{m}_{vap}$ is the water vapor mass transfer rate between muscle and

environment, Kg/s, A is the area of exposed muscle to the environment, m^2, M_{H_2O} is the water molar mass, g/mol, M_a is the dry air molar mass, g/mol, ρ_a is the dry air density, Kg/m^3, x_w is the molar fraction of water in the cardiac surface, P_{sat} is the saturation pressure of the water vapor at the element temperature, N/m^2, x_∞ is the molar fraction of water in the environment, ϕ is the humidity of the operating room, D is the mass diffusivity of water vapor on air, m^2/s, $\overline{Sh}_L$ is the average Sherwood number for the mass transfer, Sc is the Schmidt number and U_∞ is the average humid air velocity flowing just above the exposed heart, m/s.

$$\dot{Q}_{vap} = h_{fg}.\dot{m}_{vap}, \text{ where } \dot{m}_{vap} = \bar{h}_m A(\rho_w - \rho_\infty) \tag{11}$$

$$\rho_w = M_{H_2O}\frac{\rho_a}{M_a}x_w, \text{ where } x_w = \frac{P_{sat}}{1.0133x10^5} \tag{12}$$

$$\rho_\infty = M_{H_2O}\frac{\rho_a}{M_a}x_\infty, \text{ where } x_\infty = \frac{\phi P_{sat}}{1.0133x10^5} \tag{13}$$

$$\bar{h}_m = \frac{D}{d_i}\overline{Sh}_L, \text{ where } \overline{Sh}_L = 0.664Sc^{1/3}Re_L^{1/2} \text{ and } Re_L = \frac{U_\infty d_i}{\nu_a} \tag{14}$$

Finally, for obtained the numerical solution using numerical integration, a system with N ordinary differential equations was formed, with the temperatures T_i in the center of the volume elements as the unknowns of this system. Starting with initial known boundary conditions, the solution is calculated until steady state is reached using the forth order adaptive step Runge-Kutta method (Kincaid and Cheney, 1991).

3. EXPERIMENTAL VALIDATION AND RESULTS

The temperature distribution of the heart´s surface of two male patients with an average age of 62 years were evaluated during a bypass surgery using a SAT S160 infrared camera. Also, it was evaluated their corresponding coronary LAD blood flow using an ultrasonic device. Both patients had problems in at least two branches of their coronaries, and for that reason were submitted to graft bypass cardiac surgery. The camera was fixed in the vertical stand, focused directly over the exposed heart, in a way that the temperature could be easily measured and stored, as is showed in Fig. 2.

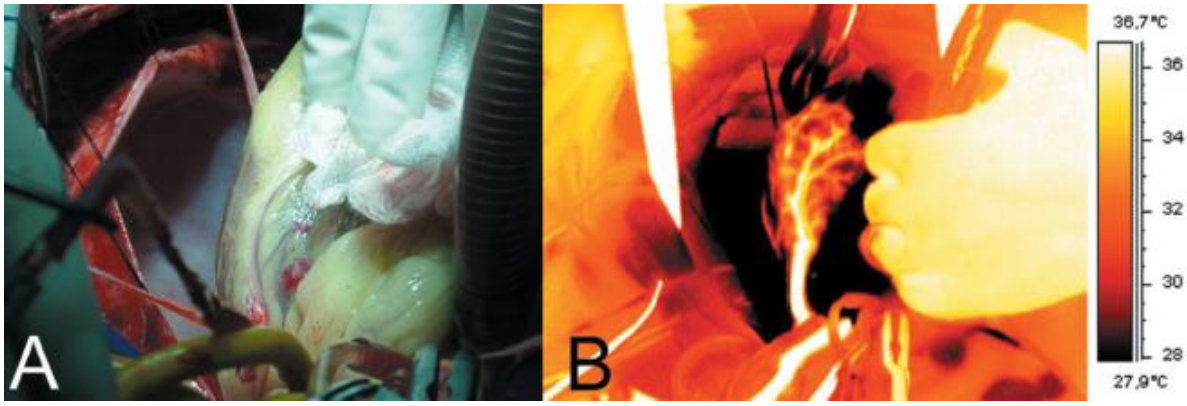

Figure 2. Normal view (a) and Infrared View (b) of the exposed heart

After that, using the exact value of measured coronary blood flow, operating room temperature and humidity, and patient temperature, the simulation was run with a converged mesh of 2,744 volume elements (14 divisions in the x direction, 14 divisions in the y direction and 14 divisions in the z direction). This mesh was compared with a refined mesh of 10,648 elements (22 divisions for each direction) and the criteria was to calculate the relative error between the module of the temperatures of both meshes, and establish that the less refined mesh had an error lower than 5%

compared to the most refined one, thus being accepted as the main mesh for all calculations. The results of the output of the computational model graphical interface for temperature distribution at some chosen planes can be seen on Figs. 3 and 4.

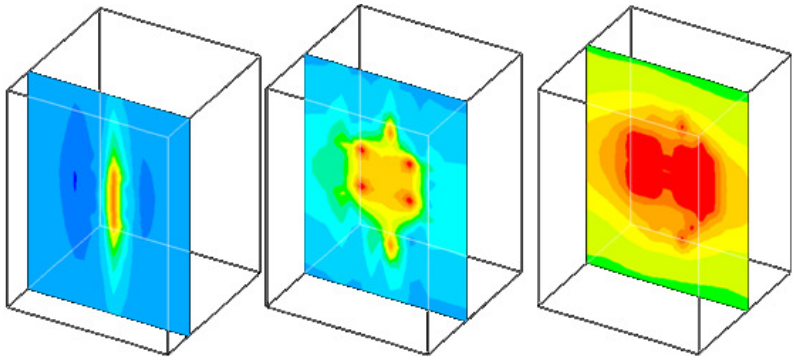

Figure 3. Computational output of 14x14x14 mesh for planes z=5, z=9 and z=12

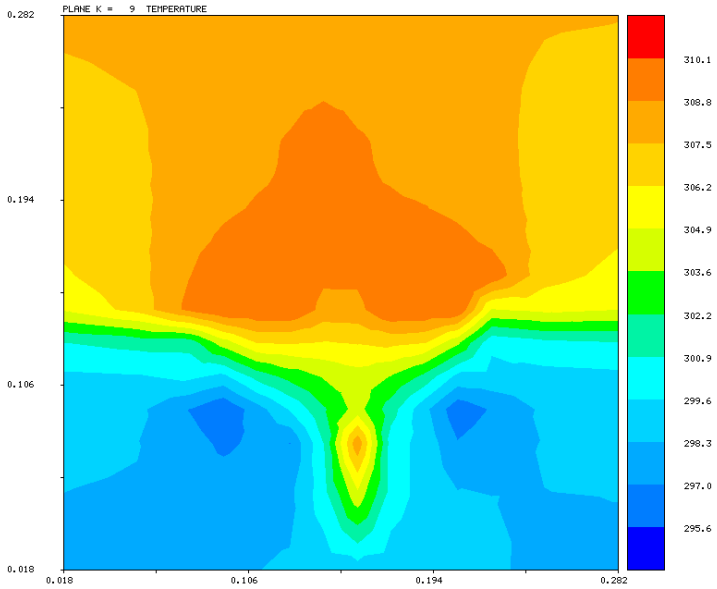

Figure 4. Bi-dimensional computational output of 14x14x14 mesh for plane x=9

For the comparisons between real temperature distribution and calculated temperature distribution over a line in the coronary vessels, a normalized value of the temperature, θ, will be used, according to Eq. (15), where T_∞ is the operating room temperature, K, and T_b is the patient body temperature, K.

$$\theta = \frac{T - T_\infty}{T_b - T_\infty}, \tag{15}$$

The normalized uncertainties of the measurements, U_θ / θ, were calculated according to Eq. (16) (ASME editorial, 1993), where B_T is the intrinsic error of the infrared acquisition equipment, defined by the manufacturer as ±0.1 K, P_T is the accuracy limit of the measurements, calculated as two times the standard deviation of three different measurements made at intervals of 1 second, K.

$$\frac{U_\theta}{\theta} = \sqrt{\left(\frac{P_T}{T - T_\infty}\right)^2 + \left(\frac{B_T}{T - T_\infty}\right)^2}, \text{ where } \frac{P_T}{T - T_\infty} = \frac{2\sigma_T}{T - T_\infty} \tag{16}$$

The numerical results were obtained for two different scenarios: 1) With normal blood flow; and 2) With obstructed flow in the LAD branch. Consequently, it was possible to directly compare the temperatures at strategic points inside the domain, calculated with the computational code, and measured during the surgery with the infrared camera.

Table 1 presents the comparison of the normalized temperatures between the computational model and the real surgery data for normal blood flow. For this surgery and consequently for the simulation, T_b=309.65 K and T_∞=295.55 K. The chosen points for comparison were the value of 10 temperature spots just above the LAD artery branch, with normal blood flow of 8.8 cm/s. X, Y and Z are the spatial coordinates of each measured and simulated spot, m, T is the temperature calculated in the simulation for that spot, K, θ is the normalized temperature of the simulation, $\overline{T}$ is the average value for 3 measurements with the infrared camera on that spot, K, $\overline{\theta}$ is the average value of the normalized measured temperature, $U_\theta / \overline{\theta}$ is the normalized uncertainty of the measure temperature.

Table 1. Comparison of normalized temperature above the LAD branch for normal blood flow

Spot Number	X (m) Position	Y (m) Position	Z (m) Position	T (K) Simulation	θ Simulation	$\overline{T}$ (K) Measured	$\overline{\theta}$ Measured	$U_\theta / \overline{\theta}$ Measured
1	0.158	0.126	0.29	308.0703	0.887965	307.1	0.819149	0.079823
2	0.158	0.094	0.27	307.9782	0.881435	306.8	0.797872	0.111377
3	0.158	0.078	0.25	308.0634	0.887479	307.1	0.821513	0.087332
4	0.158	0.078	0.23	308.4656	0.916003	307.4	0.84279	0.093075
5	0.158	0.078	0.21	308.5138	0.919419	307.4	0.84279	0.103179
6	0.158	0.078	0.19	308.4671	0.91611	307.4	0.840426	0.094349
7	0.158	0.078	0.17	308.0793	0.888603	307.1	0.821513	0.087332
8	0.158	0.094	0.15	308.1214	0.891593	307.1	0.821513	0.087332
9	0.158	0.11	0.13	308.1176	0.891321	307.1	0.821513	0.087332
10	0.158	0.126	0.11	307.9446	0.879055	306.8	0.797872	0.111377

The plotted data of Tab. 1 can be observed on Fig. 5, where can the noticed the clear comparison between the non-dimensional simulated and measured temperatures, with its respective uncertainties for each measurement.

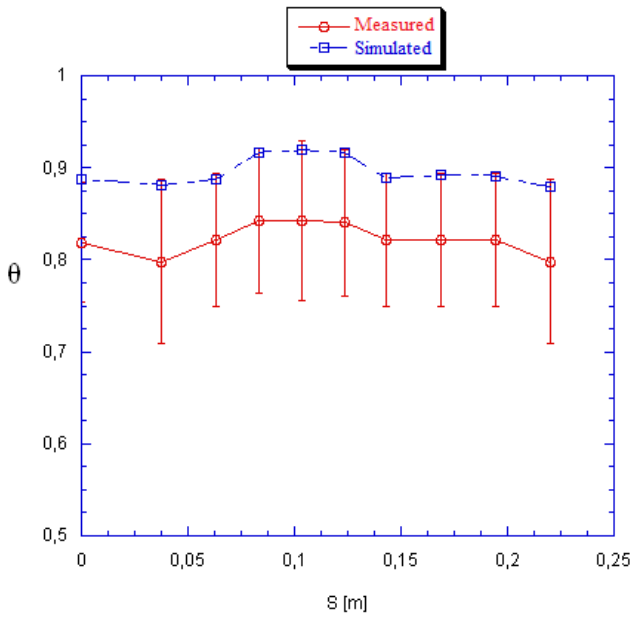

Figure 5. Comparison between calculated and measured temperature for normal blood flow

Now, the second scenario of coronary obstruction was also compared between real surgery and mathematical simulated model. Table 2 presents the comparison of the normalized temperatures between the computational model and the real surgery data for obstructed LAD blood flow. For this surgery and consequently for the simulation, T_b=309.65 K and T_∞=290.35 K.

Table 2. Comparison of normalized temperature above the LAD branch for obstructed blood flow

Spot Number	X (m) Position	Y (m) Position	Z (m) Position	T (K) Simulation	θ Simulation	$\overline{T}$ (K) Measured	$\overline{\theta}$ Measured	$U_\theta / \overline{\theta}$ Measured
1	0.158	0.126	0.29	297.7748	0.384703	297.5	0.370466	0.140558
2	0.158	0.094	0.27	294.4389	0.211862	293.6	0.170121	0.368431
3	0.158	0.078	0.25	293.1676	0.145991	292.7	0.121762	0.559699
4	0.158	0.078	0.23	293.9482	0.186437	293.6	0.168394	0.224003
5	0.158	0.078	0.21	294.1182	0.195246	294.0	0.189119	0.275339
6	0.158	0.078	0.19	293.8617	0.181954	293.3	0.15285	0.246783
7	0.158	0.078	0.17	292.9712	0.135814	292.8	0.125216	0.375466
8	0.158	0.094	0.15	294.2784	0.203544	294.2	0.199482	0.139874
9	0.158	0.11	0.13	295.4353	0.263492	295.4	0.259931	0.085350
10	0.158	0.126	0.11	296.5529	0.321395	296.7	0.330743	0.101928

Again, the plotted data of Tab. 2 can be observed on Fig. 6, where can the noticed the clear comparison between the non-dimensional simulated and measured temperatures, with its respective uncertainties for each measurement.

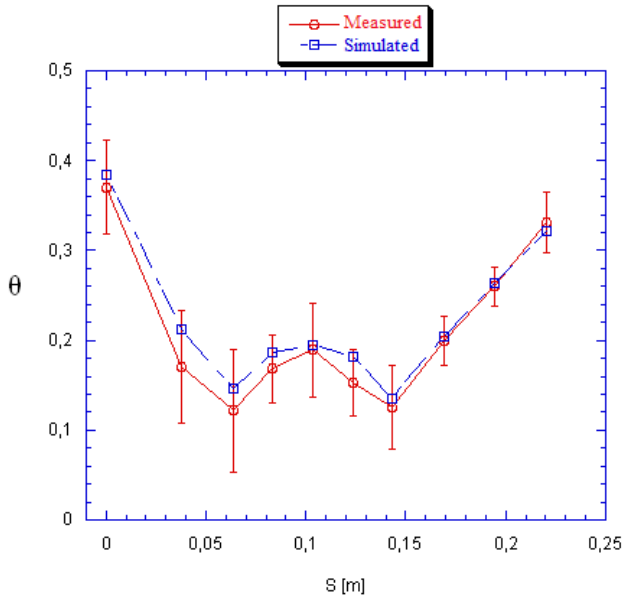

Figure 6. Comparison between calculated and measured temperature for obstructed LAD blood flow

4. CONCLUSIONS

The comparisons presented on Figs. 5 and 6 are a good indication that the computational simulation reproduces approximately the real behavior of proposed domain, thus validating the numerical model developed.

As it could be noticed in the presented paper, the tridimensional method of volume elements takes account the association of various thermodynamics transfer mechanisms, such as conduction, natural convection, forced convection and also the latent heat of vaporization of the water in the surface of the cardiac muscle. It is expected that this model can turn into a powerful simulation tool for calculating the temperature distribution of the complete heart, thus giving the surgeon means to predict temperatures for heart conservation and extra-corporeal circulation based on the obstruction level of the coronaries branches.

As the computational time for solving the complete temperature distribution of the heart took approximately 10 minutes for this model, it is suggested to aim for a parallel computing method that takes even less computional time, which will be pursued in the next versions of this model. Also, it is important to state that the motivation of this work was to present a realistic model that can be used for the inverse problem solution, which is to calculate the coronary blood flow based on the heart´s temperature distribution acquired with the infrared camera. This way, the correct reperfusion bypass procedure could be evaluated in real time during the surgical procedure, thus providing the surgical team with a more concrete way to be sure that the new heart´s flows and perfusions are according the expected values.

5. REFERENCES

ASME Journal of Heat Transfer, Journal of Heat Transfer Policy on Reporting Uncertainties in Experimental Measurements and Results, Editorial, V. 115, p. 5-6, 1993

Bejan, A. Convection Heat Transfer, 2. Ed. New York: John Wiley & Sons, 1995a

Bejan, A. Heat Transfer, X Ed. New York: John Wiley & Sons, 1993

Churchill, S. W. and Chu, H. H. S. Correlating equations for laminar and turbulent free convection from a vertical plate, International Journal of Heat Mass Transfer, V.18, p. 1323-1329, 1975

Fletcher, C. A. J. Computational Techniques for Fluid Dynamics, Vol. 1, X Ed. Berlim: Springer-Verlag, 1991.

Gordon, N., Rispler, S., Siderman, S., Shofty, R., Beyar, R., Thermographic imaging in the beating heart: a method for coronary flow estimation based on a heat transfer model, Medical Engineering & Physics 20, 1998, pg. 443-451.

Kincaid, D. and Cheney, W. Numerical Analysis, X Ed. Belmont CA: Wadsworth, 1991.

Papp, L., ALLO, G., Kekeshi, V., Juhasz-Nagy, A., Correlation between coronary flow and epicardial temperature determined by quantitative infra-red thermography. IRCS Med Sci 1985. 13:621-2.

Robicsek F, Masters TN, Svenson RH et al, The application of thermography in the study of coronary blood flow. Surgery 1978; 84: 858-64.

Sterk, M., Trobee, R., Biomedical Simulation of Heat Transfer in a Human Heart, J. Chem. Inf. Model., 2005, 45, p. 1558-1553.

Vargas, J. V. C., Ordonez, J. C., Bejan, A. , Constructal flow structure for PEM Fuel Cell, International Journal of Heat and Mass Transfer , V. 47, p. 4177 - 4193, 2004.

Vargas, J. V. C. and Bejan, A. , Thermodynamic optimization of internal structure in a fuel cell, International Journal of Energy Research, V. 28, n.4, p. 319 - 339, 2004.

6. RESPONSIBILITY NOTICE

The authors are the only responsible for the printed material included in this paper.